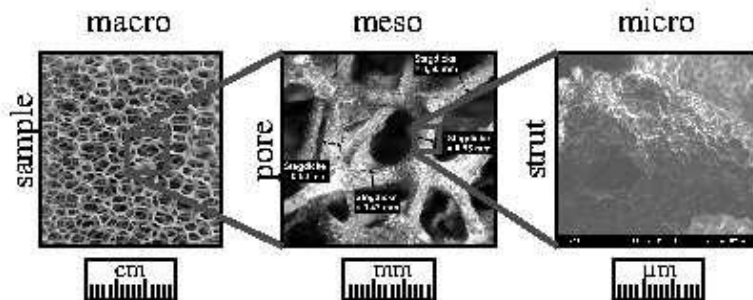


Generation of open foam RVEs with sharp edges using Distance fields and Level sets

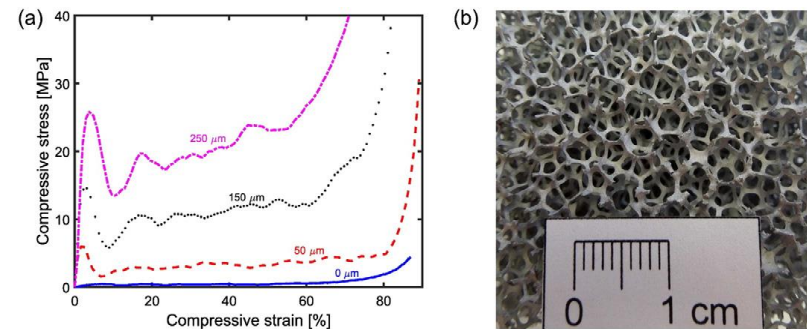
Computational Modeling and Analysis of
Complex Cellular Material RVEs

Nanda G. Kilingar
K. Ehab Moustafa Kamel
B. Sonon
L. Noëls
T.J. Massart

- **Metallic open foams**
 - Low density
 - Novel physical, mechanical and acoustic properties.
 - Offer potential for lightweight structures, with high stiffness and energy absorption capability.
 - With advancing manufacturing capabilities, they are becoming more affordable.
- **Properties and applications results from chemical and physical properties of the bulk material and cell structure.**
- **Ability to model 3D foams based on actual foam samples**
 - Helps in characterization
 - Stochastic approaches and multi-scale mechanics used to simulate the behavior



Jung & Diebels 2014



Jung et al 2015

Open foam properties

- Manufacturing (Zhou et al 2002)

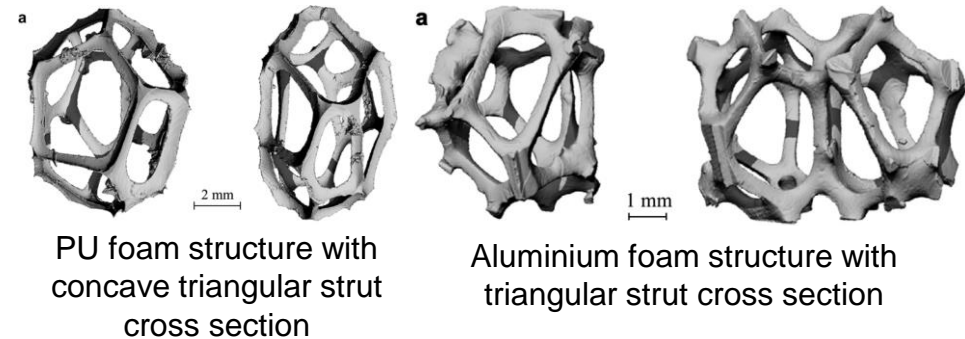
- PU foam → phenomenon of bubble expansion
- Metallic foam → PU foams + casting/electrodeposition

- Plateau's law (Sonon et al 2015)

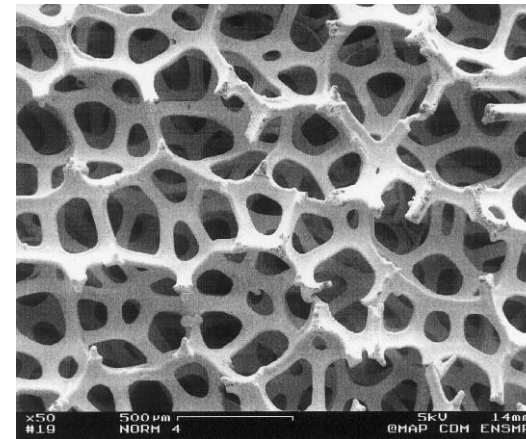
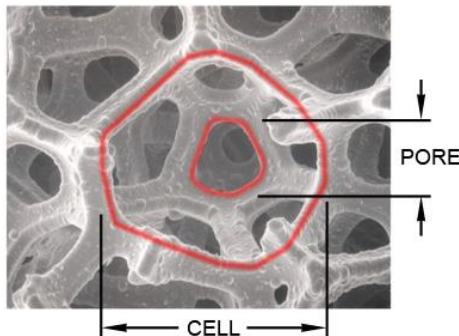
- Soap bubble → Plateau's law, Surface energy minimization
 - Constant mean curvature of each face
 - 3 faces meet at 120° , equal dihedral angles
 - 4 edges join at equal tetrahedral angles (109.47°)



Cross section of the struts of open-cell foam commercially manufactured by ERG under Duocel trademark; percentage refers to the resulting relative density



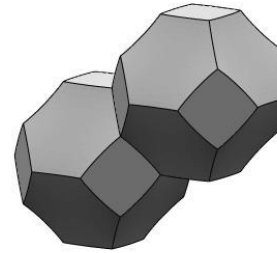
Jang et al (2008)



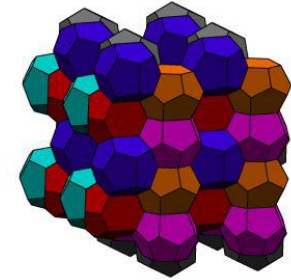
Nickel open-cell foam;
Badiche et al (2000)

- Regular models

- Kelvin's tetrakaidecahedra (1887)
- Weaire-Phelan cell (1993)
 - These models are too regular and fail to represent foams with non-uniform bubble sizes and out-of-equilibrium solid foams.



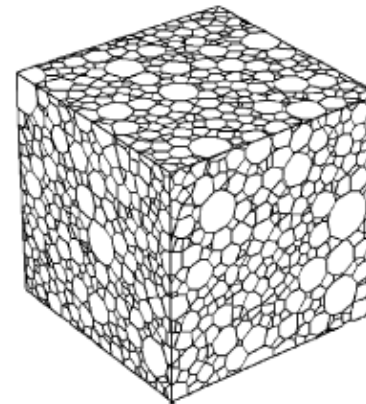
Kelvin cell



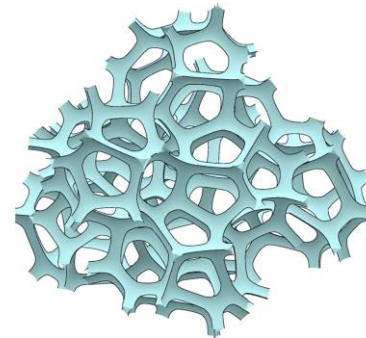
Weaire-Phelan modification

- Tessellations of sphere packing distribution – Laguerre tessellations

- Sphere packing generation
 - Concurrent or force-biased approach (Ex, Stroeven 1996)
 - Sequential approach (Ex, RSA, Cooper 1988)
- Tessellation generated by methods like convex hull (QHull, Barer et al 1996)
- Morphological parameters like face-by-cell count, edge-by-face count, interior angles match very well



Random close packing of spheres based Laguerre Voronoï diagram (Fan et al 2004)

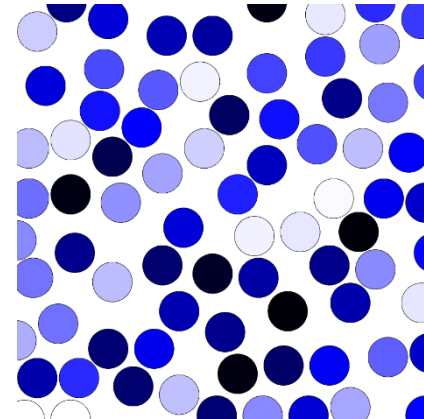


Soap bubble based model by Surface Evolver (Jang et al 2008). This process is complex and time-processor intensive

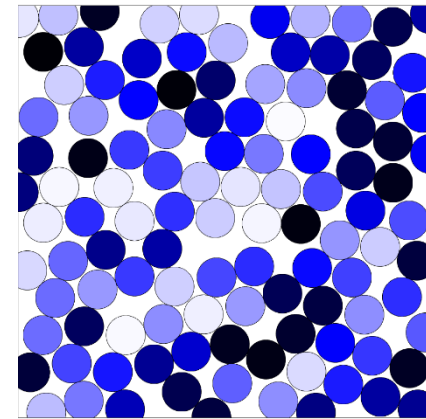
- DN-RSA based packing generation
 - DN-RSA Notation
- Tessellation Generation
- Open foam morphology
- Sharp Edge extraction
 - Multiple level set method
 - Inner level set extraction
 - 3D Open Foam model
- Properties of the RVEs generated
 - Strut cross-section variation
- Linear elasticity sample study
- Limitations and advantages

DN-RSA based packing generation

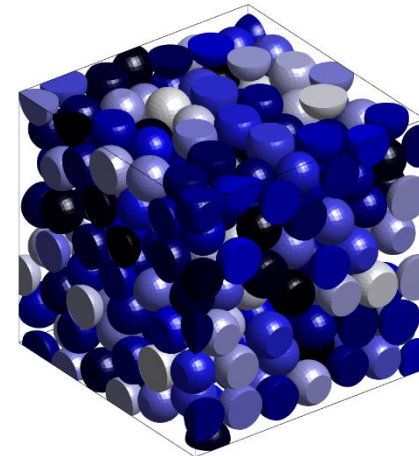
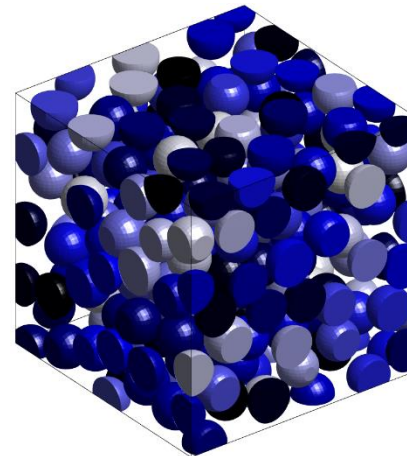
- Method to generate random arbitrary shaped inclusion packing based on distance neighbors (Sonon 2012)
 - Packing with no constraints between individual inclusions – Random sequential addition (RSA)
 - Constraints based on distance from nearest neighbors to generate the most optimal packing – DN-RSA
 - Limit of vanishing discretization size \rightarrow Most optimal packing
 - Computational cost of the method is linear due to the control on neighboring distances
 - Can generate periodic packings as well as packings with free boundaries
 - Packing fraction of the spheres and distribution of the volumes of the spheres can be controlled to obtain a wide range of packings



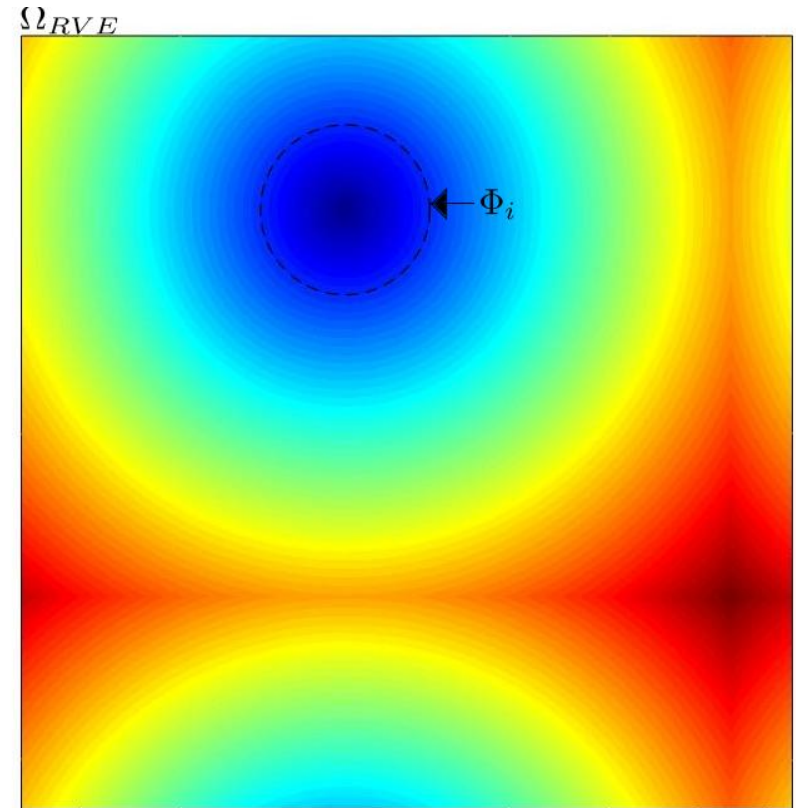
RSA packing



DN-RSA packing

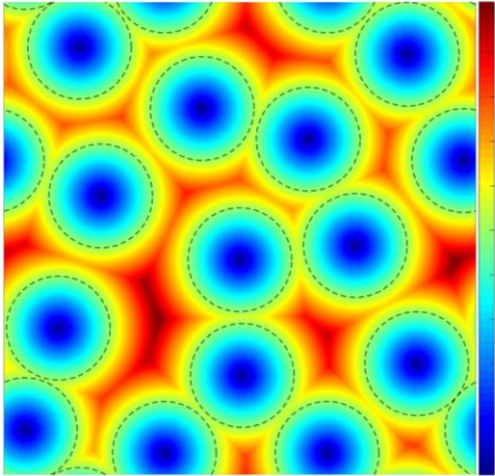


- Inclusions from desired distribution/shape are generated and placed in the domain.
 - Each grid point assigned a $DN_k(\mathbf{x})$ value, k - the k th nearest inclusion to the given point.
- $DN_k(\mathbf{x})$
 - negative inside the inclusion
 - positive outside.
- With addition of more inclusions, the $DN_k(\mathbf{x})$ value gets updated, depending on the k -th nearest inclusion and this inclusion mapping is stored as $NN_k(\mathbf{x})$.

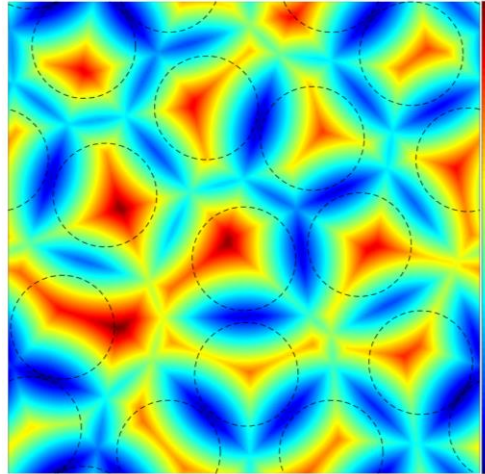


$DN_1(\mathbf{x})$ plot with only 1 inclusion

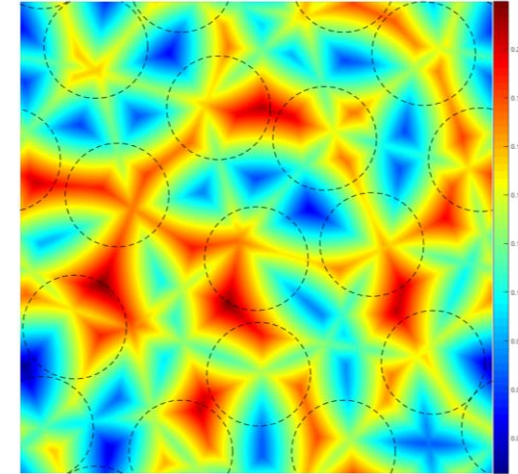
- $DN_k(\mathbf{x})$ is the k-th neighbor distance field



$DN_1(\mathbf{x})$

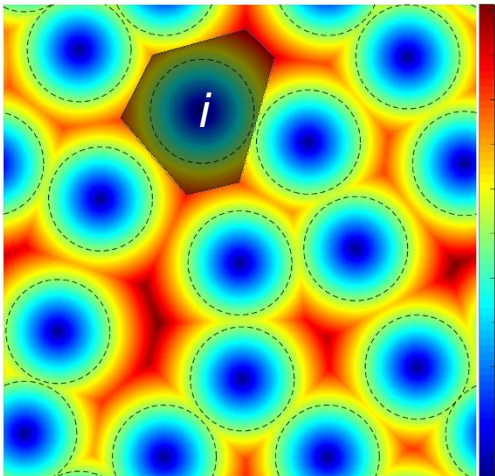


$DN_2(\mathbf{x})$

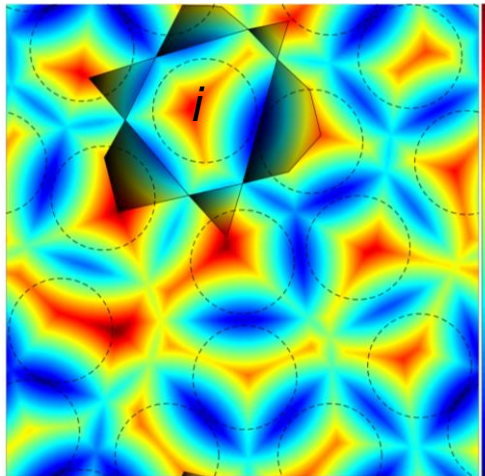


$DN_3(\mathbf{x})$

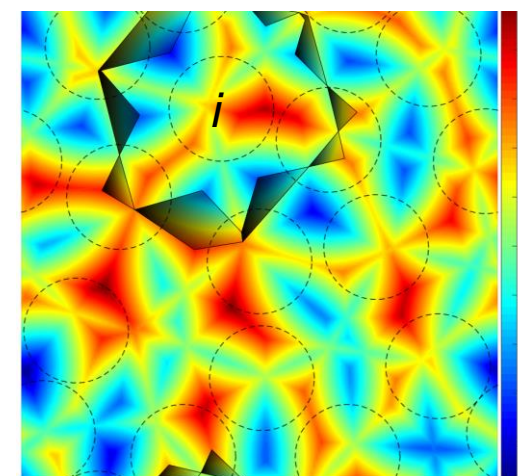
- $NN_k(\mathbf{x})$ is the k-th neighbor identity map



$NN_1(\mathbf{x}) = i$



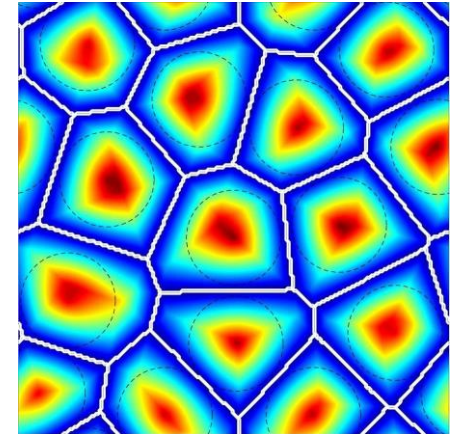
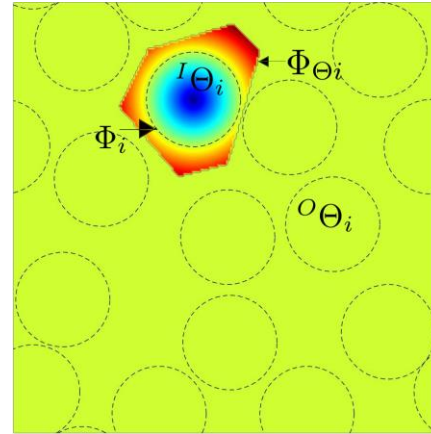
$NN_2(\mathbf{x}) = i$



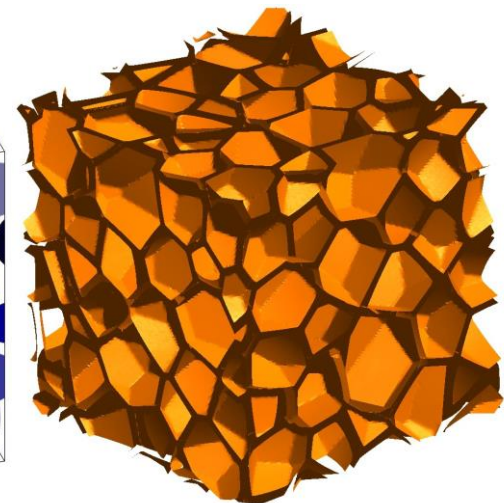
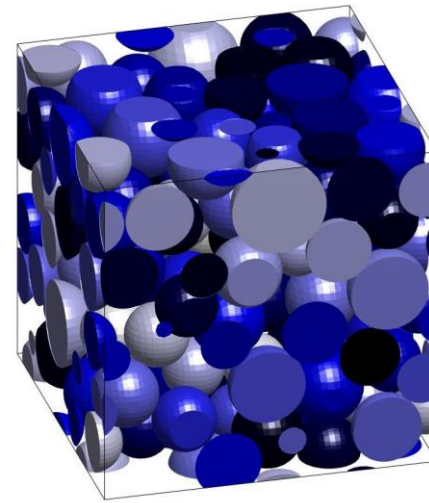
$NN_3(\mathbf{x}) = i$

- Tessellation

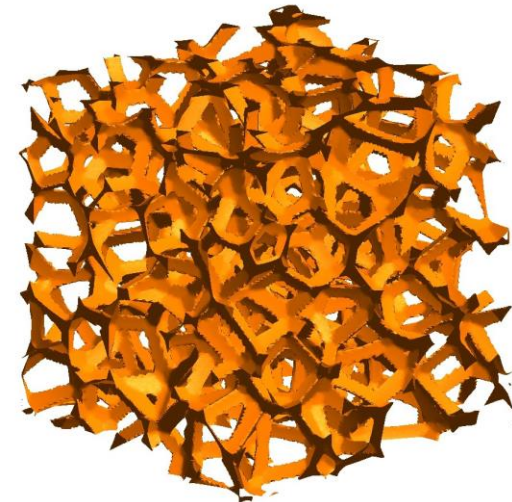
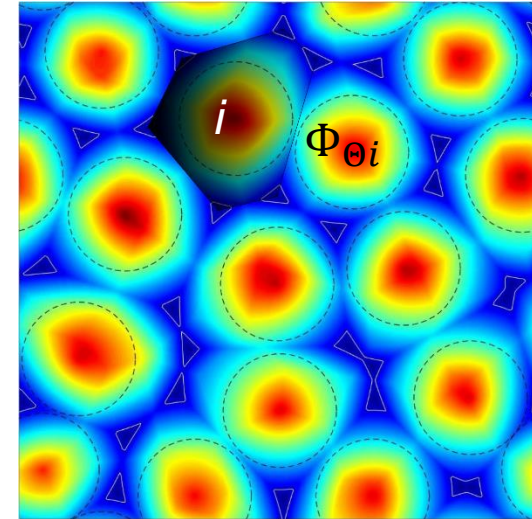
- Assembly of all domains I_{Θ_i} that enclose, for each inclusion i , points closer to this inclusion than to others, i.e., $NN_1(\mathbf{x}) = i$.
- Φ_i , the boundary of the sphere
- Φ_{Θ_i} , the boundary of the tessellation
- O_{Θ_i} , the domain where the closest inclusion is not i , i.e., $NN_1(\mathbf{x}) \neq i$.



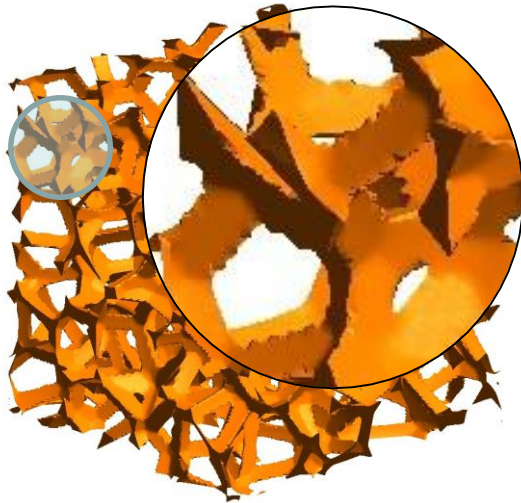
- Implicitly extracted in DN-RSA by “Voronoi” level set function:
 - $O_V(\mathbf{x}) = DN_2(\mathbf{x}) - DN_1(\mathbf{x})$
- Quasi-constant thickness, closed cell geometry through level-sets can then be extracted:
 - $O_v(\mathbf{x}) - t = 0$



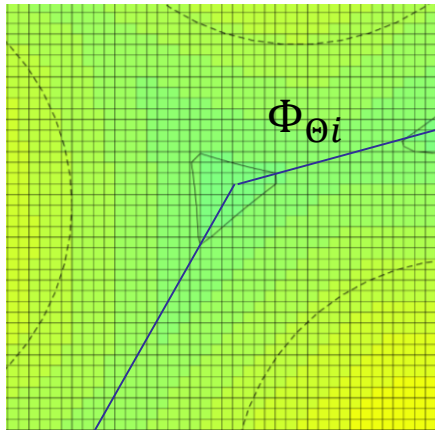
- Plateau borders in liquid foams form at the intersection of three films. Thus we combine the 3 first neighbor distance functions.
- “Plateau” Level set function
 - $O_P(\mathbf{x}) = \frac{DN_3(\mathbf{x}) + DN_2(\mathbf{x})}{2} - DN_1(\mathbf{x})$
- Function consists of triangles with vertex lying on the tessellation cell boundaries.
- Thus, we can extract plateau border like geometry through
 - $O_P(\mathbf{x}) - t = 0$
 - Parameter t used to control thickness of extracted borders



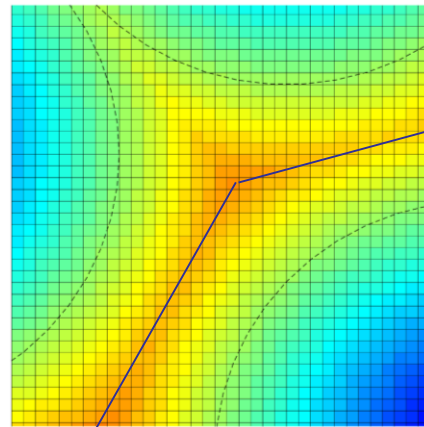
Sharp edge extraction



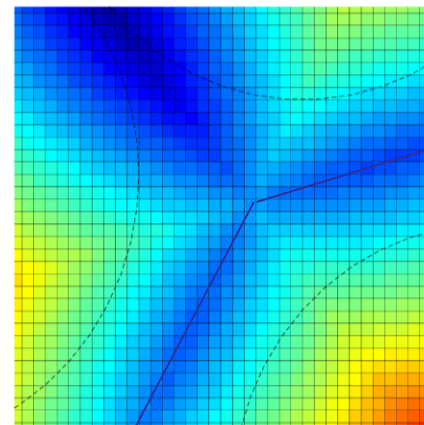
- Plateau borders present sharp edges due to their triangular prism shape
 - Origin is due to steep discontinuity of $DN_k(\mathbf{x})$ derivatives on Φ_θ
- Single level set function can not represent this with discrete level set functions, and we need multiple level set function strategy



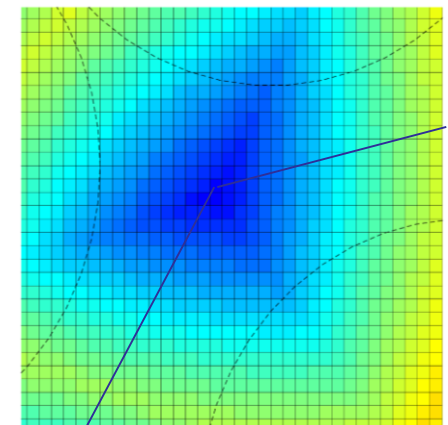
t Level Set



$DN_1(\mathbf{x})$



$DN_2(\mathbf{x})$

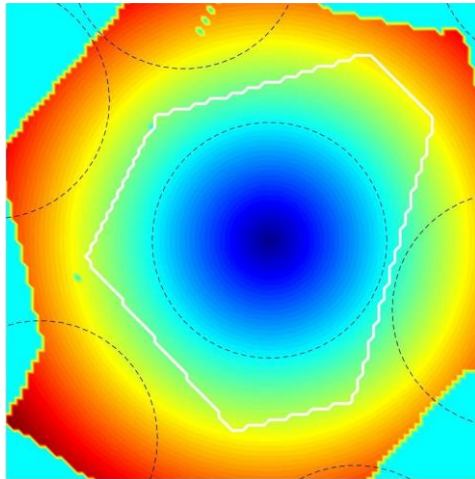


$DN_3(\mathbf{x})$

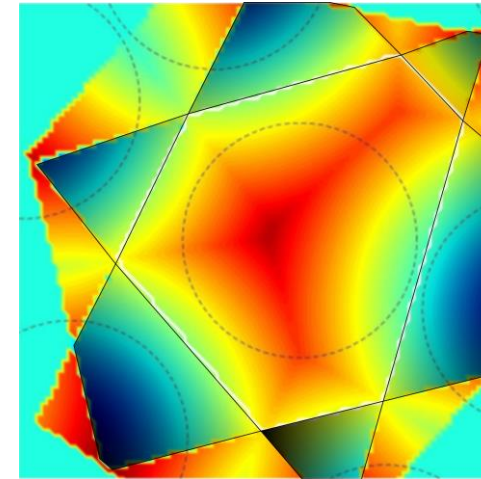
Clipping of the triangular section at grid positions and the presence of discontinuities in $DN_1(\mathbf{x})$ and $DN_2(\mathbf{x})$ across Φ_θ . $DN_3(\mathbf{x})$ is continuous.

Sharp edge extraction – Multiple level set functions

- Local level set functions for each inclusion, ${}^I O_P(\mathbf{x}) \rightarrow$ Global “Plateau” function, $O_P(\mathbf{x}) +$ modified $DN_k(\mathbf{x})$
 - Local functions are built for each inclusion from modified $DN_k(\mathbf{x})$, called ${}^I DN_{ki}(\mathbf{x})$ only in the domain $NN_k(\mathbf{x}) = i$, $k = \{1,2,3\}$.

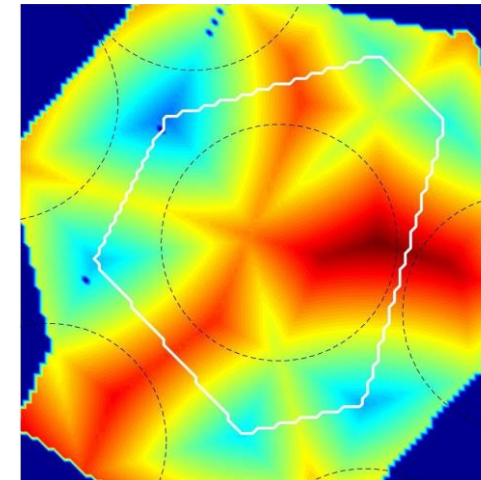


${}^I DN_{1i}(\mathbf{x}) = DS_i(\mathbf{x})$
 $DS_i(\mathbf{x})$ is the signed distance field of the domain for inclusion i



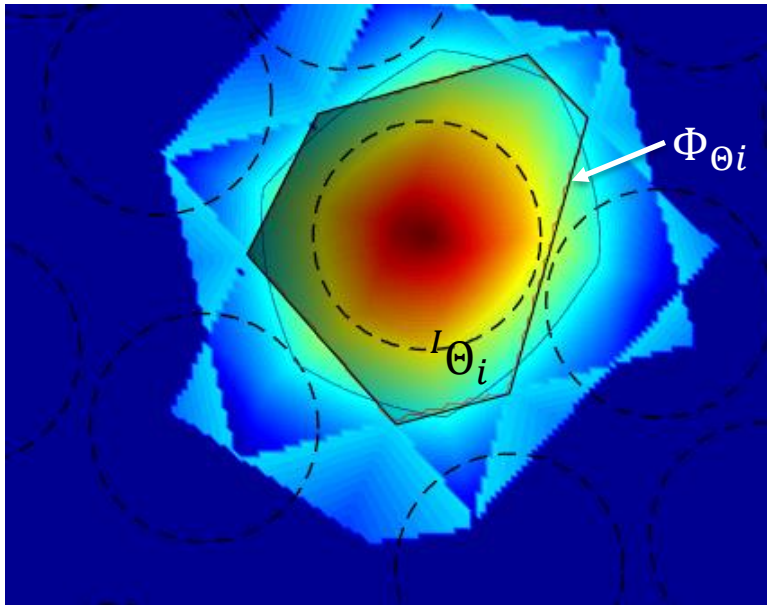
$${}^I DN_{2i}(\mathbf{x}) = \begin{cases} DN_2(\mathbf{x}), & NN_2(\mathbf{x}) \neq i \\ DN_1(\mathbf{x}), & NN_2(\mathbf{x}) = i \end{cases}$$

$NN_2(\mathbf{x}) = i$ is the shaded domain

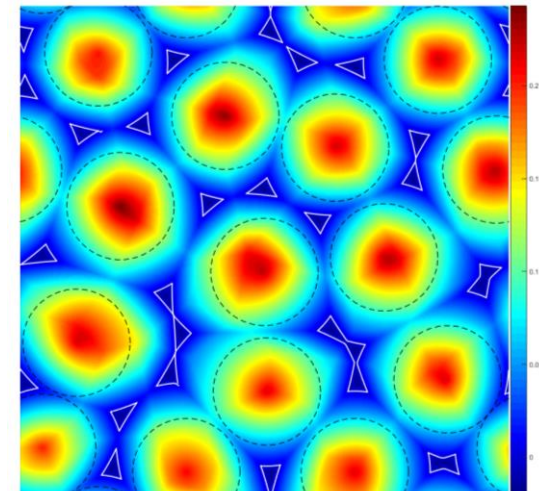
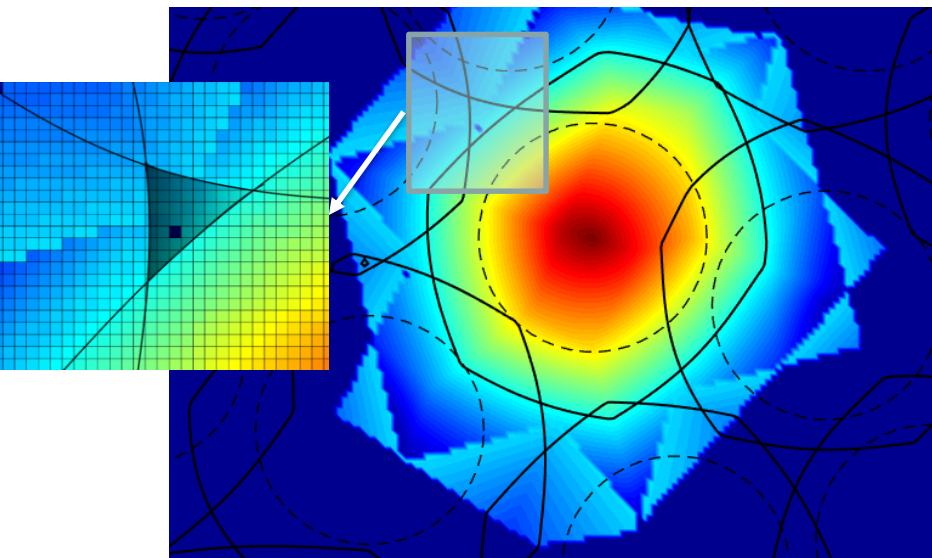


${}^I DN_{3i}(\mathbf{x}) = DN_3(\mathbf{x})$
 $DN_3(\mathbf{x})$ is continuous across Φ_θ

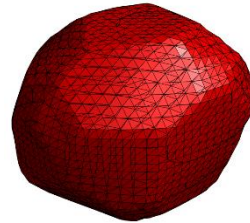
Sharp Edge Extraction – “Inner” Level Set function



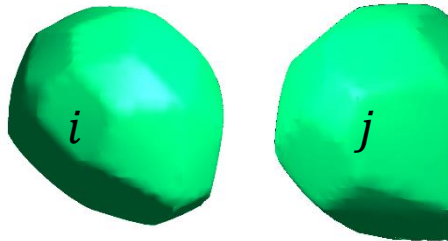
- ${}^I O_{Pi}(x)$ function, with t level set, C^1 continuous across Φ_{Θ_i} and equal to global function $O_P(x)$ in domain ${}^I \Theta_i$.
- The value of ${}^I O_{Pi}(x)$ is positive towards the center of the inclusion and negative outside.
- The t level set is stored for individual inclusion.
- The t level set of inclusion i is iteratively compared with t level sets of the neighboring inclusions.
- Segments of t lying such that ${}^I O_{Pj}(x) > 0, j \neq i$ are sliced off.



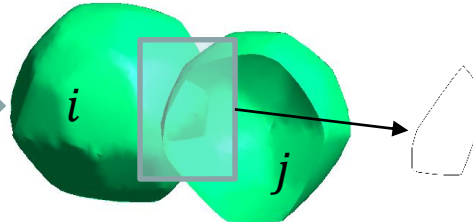
Sharp Edge extraction



t level set of inclusion i
extracted in MATLAB using
isosurface function



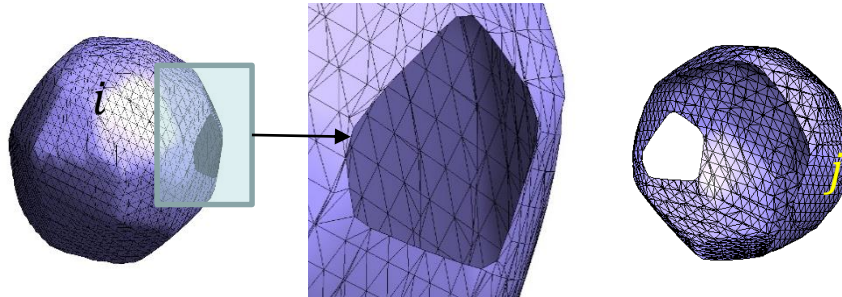
Intersection of t
level sets of
inclusion i and j



Extract, re-mesh and
fix the line of
intersection

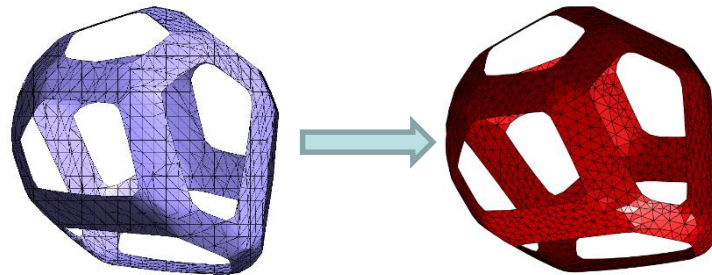


Slice-off the elements
lying in the domain
 ${}^iO_{Pj}(x) > 0, j \neq i$

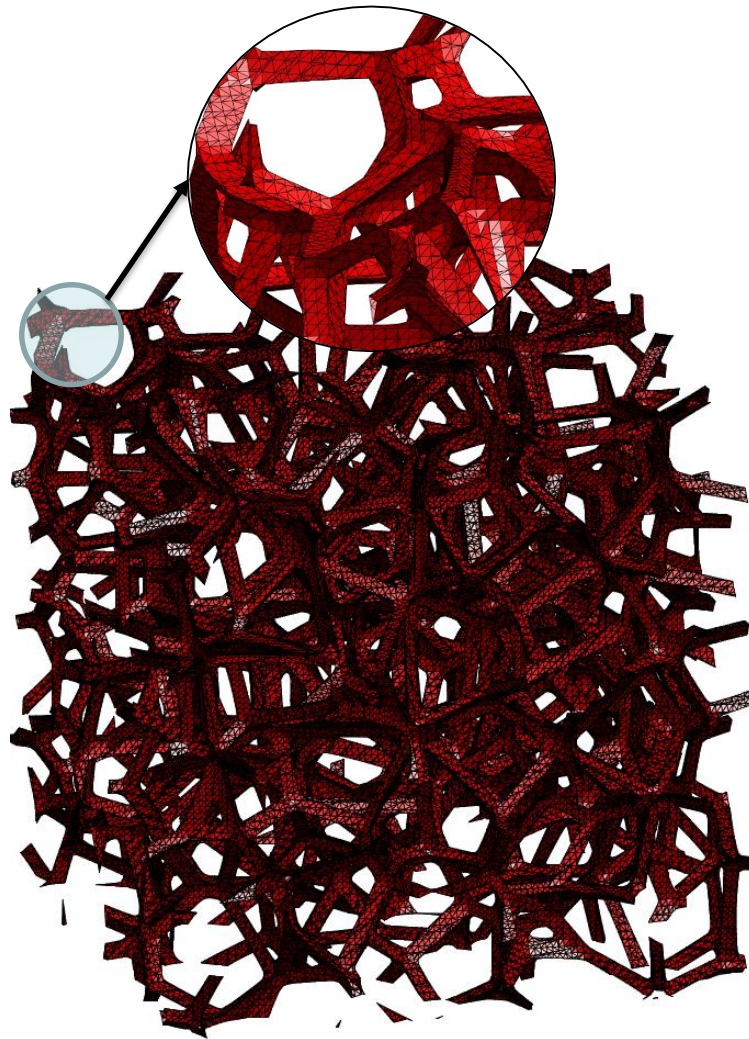


Similarly, **slice-off** the
elements of t level set
of inclusion j lying in
the domain ${}^iO_{Pi}(x) > 0, i \neq j$

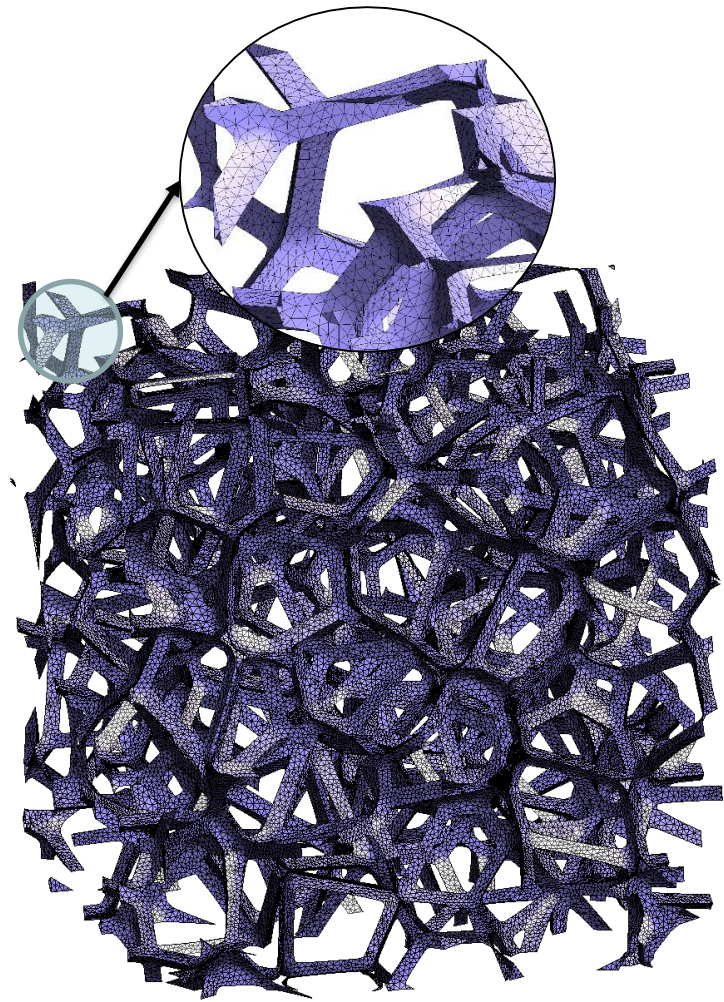
Iteratively done, leaving
only the plateau border
part of the inclusion.



Inclusions are then refined by the
approach designed by [Karim et
al 2017] before assembling. 3D
mesh is generated using Tetgen
(Hang Si 2015)



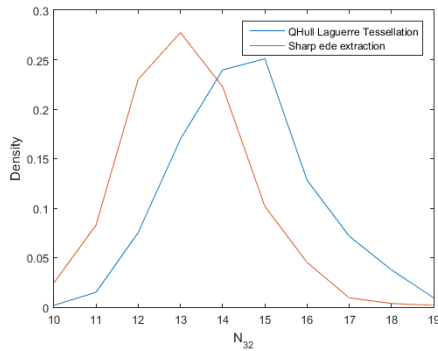
Assembly of all inclusions after sharp edge extraction



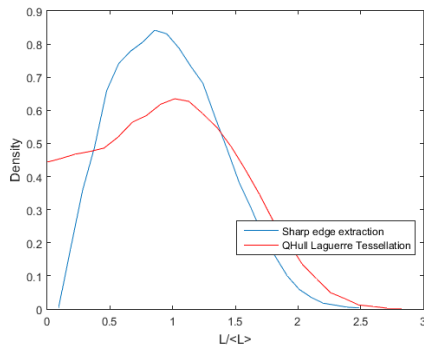
Assembly of all inclusions after remeshing, the surface elements have been processed to make the mesh more uniform

Properties of the RVE generated

Comparison between QHull Laguerre model and DN-RSA model

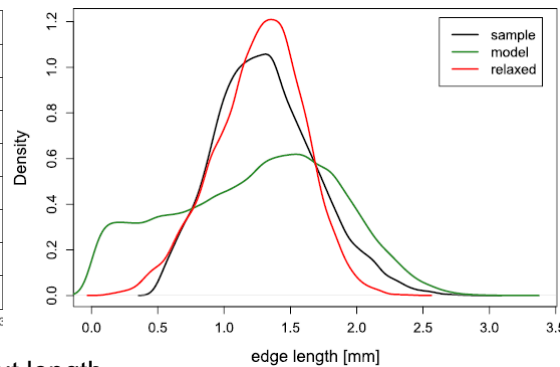
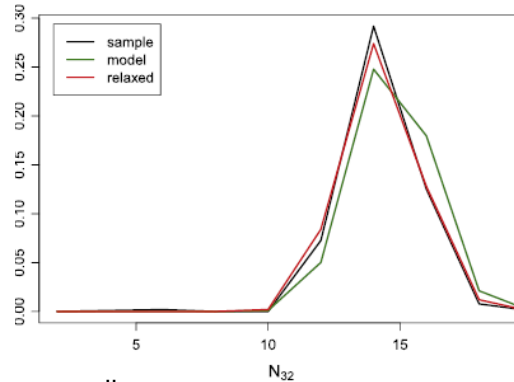


No. of faces per cell



Strut length

Comparison between AI foam sample, QHull Laguerre model and Surface Evolver based model fitted to AI foam; Vecchio et al 2016

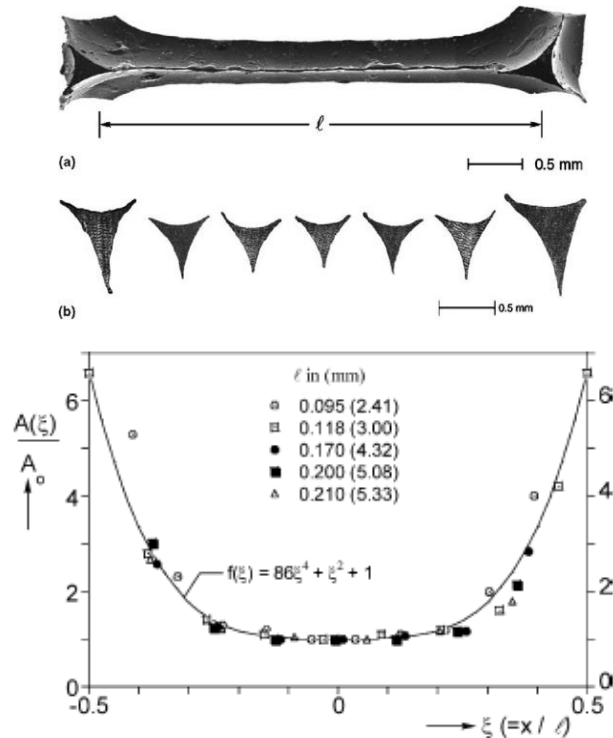


The RVEs generated have a mean face per cell value ranging from 13.5 to 14.5 depending on the packing fraction of the sphere, lower the fraction, more irregularity in the RVE.

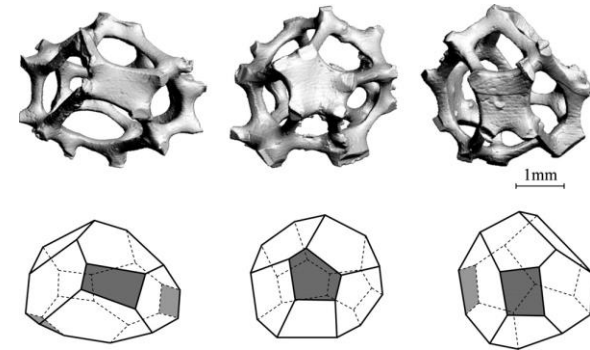
Typical high values found in Laguerre tessellations from QHull not obtained due to limitations of the discretization grid.

Strut length distribution from DN-RSA in comparison with QHull Laguerre tessellations show that the short edges get absorbed by the sharp edge extraction technique, mimicking the process of model extraction from (Van der Burg et al 1997)

Strut cross section variation



Strut cross section variation and mid-span cross-sectional area of a polyurethane foam; Gong et al 2004

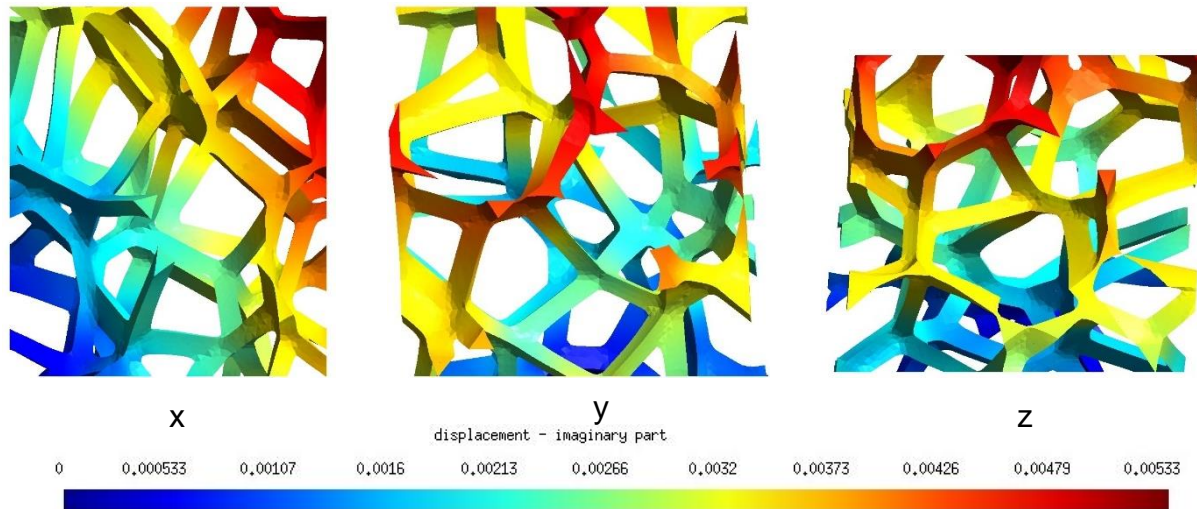


Closing of faces in metallic foam manufactured by investment casting; Gong et al 2004



Variation of relative density of the foam with varying cross section profile: plateau, triangular, casting convex triangular and circular (used in most models); Duocel™ by ERG

DN-RSA is able to incorporate these variations by modifying the “Plateau” function O_P according to the domain: Next phase of work



- Displacement analysis of an RVE of a foam generated using DN-RSA, the RVE is under tensile and shear stress.
- This shows the convenience of importing the RVE generated from DN-RSA to the solvers available with CM3 group to generate larger sized RVEs as [Stochastic volume elements](#) and analyze using multiscale techniques

- **Higher discretization** of the grid required to capture higher sphere packing
- Laguerre tessellations are known to have higher number of **small struts** and **triangular faces** that are skewed,
 - captured by DN-RSA in the limit of vanishing discretization size.
- Representation of foams with RVE having high dispersion rate of the inclusion size is difficult with this model as the purpose of multi-scale modeling is lost.
- Easy access to **the signed distance functions** allows us to implement variations in the morphology
 - strut cross-section variation at the mid-span and along the axis of the strut
 - combination of open-closed faces of tessellated cells
 - Coating of the RVE to represent realistic engineering applications
- A balance of discretization size allows us to model the foam without the issues of small/skewed faces as they are implicitly enveloped by the extracted t level set.
- Extracted mesh can be easily utilized for **a multi-scale study** and understand the effects of upscaling the model to study the elastic-plastic properties of such foams

Thank you for your attention

Generation of open foam RVEs with sharp edges using Distance fields and Level sets

Nanda G. Kilingar, K. Ehab Moustafa Kamel, B. Sonon, L. Noëls, T.J. Massart

Computational & Multiscale Mechanics of Materials – CM3

<http://www.ltas-cm3.ulg.ac.be/>

B52 - Quartier Polytech 1

Allée de la découverte 9, B4000 Liège

ngkilingar@uliege.be